Heliyon 6 (2020) e03486

Contents lists available at ScienceDirect

Heliyon

journal homepage: www.cell.com/heliyon

Research article

A comparison of chitosan properties after extraction from shrimp shells by diluted and concentrated acids

Mohammed Eddya, Bouazza Tbib, Khalil EL-Hami *

University of Sultan Moulay Slimane, Polydisciplinary Faculty of Khouribga, Laboratory of Nanosciences and Modeling, Morocco

ARTICLE INFO

Keywords:
Materials science
Chitosan
Chitin
Gap energy
Degree of deacetylation
SEM
Raman spectroscopy
FTIR
XRF
XRD

ABSTRACT

Chitosan and chitin are mainly extracted from shells of fish such as lobsters, crabs or shrimps. Originally, the raw material and the two compounds are identical. This study aims to show the acid concentration effect on chitosan extraction from shrimp shells between concentrated and diluted acid; on surface morphology, thermal resistance, structural, elemental composition, optical and opto-electronic properties. It also aims to reduce the production time and increase the quantity. We focused mainly on comparing between Physico-chemical properties of chitosans extracted by diluted (1M) and concentrated (20%) Chloric acids, and sometimes we compare by other concentrated acids like nitric acid (70%) and sulphuric acid (98%). We performed the product's characterization by various tools such as: X-ray diffraction (XRD) spectroscopy, X-ray fluorescence (XRF) analysis, UV-Visible spectroscopy, Fourier Transformed Infra-Red (FTIR), Raman Spectroscopy, Thermogravimetry and Derivative Thermogravimetry (TG/DTG), Scanning Electron Microscopy (SEM), Energy-dispersive X-ray spectroscopy (EDX) analysis. The elemental analysis (XRF and EDX). The results showed that all chitosan samples we gained are good about 80% degree of deacetylation, and pure mostly composed by carbon between (15,02% - 45.55%), nitrogen (4,17% - 12.28%) and oxygen (42.16% and 81.25%), with appearance of essential peaks for chitosan in Raman analysis: 470 cm^{-1} → ν(C-C(=O)-C), 1000 cm^{-1} → ν(C-H), 1800 cm^{-1} → δ(C=CCOOR), δ(C=O), 2630 cm^{-1} → δ(CH) rings, 3250 cm^{-1} → ν(NH_2). All our chitosan particles are ultrafine nanoscale between 8 and 34 nm.

1. Introduction

The chitosan and chitin are the most important substances in the fabric of medicines [1] and products with anti-microbial [2] and anti-bacterial properties [3], they provide anticancer activity against human monocyte leukaemia cell line [4]. Also, M. Bouhenna et al demonstrated in 2015 that chitin and its derivatives have a dose-dependent cytotoxic effect against Human larynx carcinoma cell lines and Human embryo rhabdomyosarcoma cell lines, indicating that there are several types of interactions between the charged groups of molecules and tumor cells such as electrostatic interactions between the negative charges of tumor cells groups and the positive charges of groups tested and interactions between hydrophobic groups and tumor cells derived molecules [5]. Total global production of captured and farmed shrimp reached 6 million tons in 2006 (FAO, 2009), with only 60% being used as food, leaving 2.3 million tones for non-food uses. Shrimp waste, which is rich in chitin, proteins, lipids, pigments and flavor compounds, has potential commercial value in the food industry [6]. Since their first discovery by Henri Bracannot in 1811 through their research on mushrooms till present, several major events have occurred for chitin and chitosan materials. We summarize in Figure 1, the most important events that have been achieved for chitin and chitosan by different scientists around the world in different research fields between the years 1811–1950s [7, 8, 9, 10, 11, 12, 13, 14].

Furthermore, in 1993 Rane et al [15] evaluated the alkali and acid treatments for chitosan extraction from Fungi, using sodium hydroxide with varying extraction times at 95 °C and 121 °C as alkali treatment and chloric, formic and acetic acids as acid treatment at 95 C with various extraction time durations. They concluded that the highest yields of chitosan under alkaline extraction is at 121 °C for 30 min and chloric acid extraction at 95 °C for 12 h with effects on the degree of deacetylation and viscosity of chitosan. Another study by Percot et al in 2003 [16] defined the optimal conditions to extract chitin from shrimp shells, showing the role of temperature on remains of calcium and proteins on chitin, the weight of molecules, and degrees of acetylation (DA). According to them, the elimination of minerals is complete in time duration around 15 min at home temperature with excess of chloric acid 0.25 M. The deproteinization is well obtained in 1 M of sodium hydroxide within

* Corresponding author.
E-mail address: elhami_k@yahoo.com (K. EL-Hami).

https://doi.org/10.1016/j.heliyon.2020.e03486
Received 11 December 2018; Received in revised form 11 November 2019; Accepted 20 February 2020

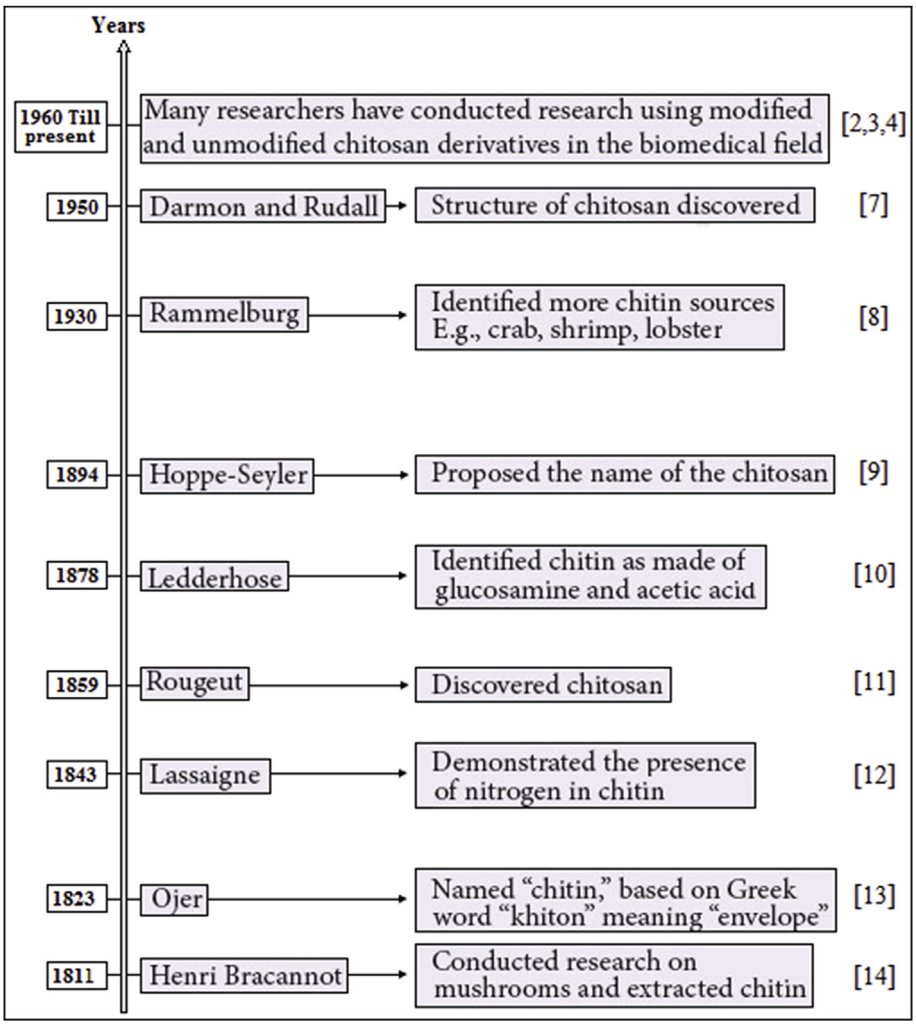

Figure 1. History of the most important events that have been achieved for chitin and chitosan between the years 1811–1950s.

24 h at 70 °C without effect on the molecular weight or the DA. In this case, the remains of calcium in chitin are under 0.01%, and the DA is about 95%. Besides, Burrows et al in 2007 [17] extracted chitosan from crab exoskeleton as a seed fungicide, using either 0.5%, chloric acid 1.0% and acetic acid 5%. The chitosan extracted with 0.5% chloric acid had the most effect in eliminating fungus and plants growth enhancer. Recently, from several studies [18, 19, 20], waste fungal biomass that results from various pharmaceutical and biotechnological industries set out a

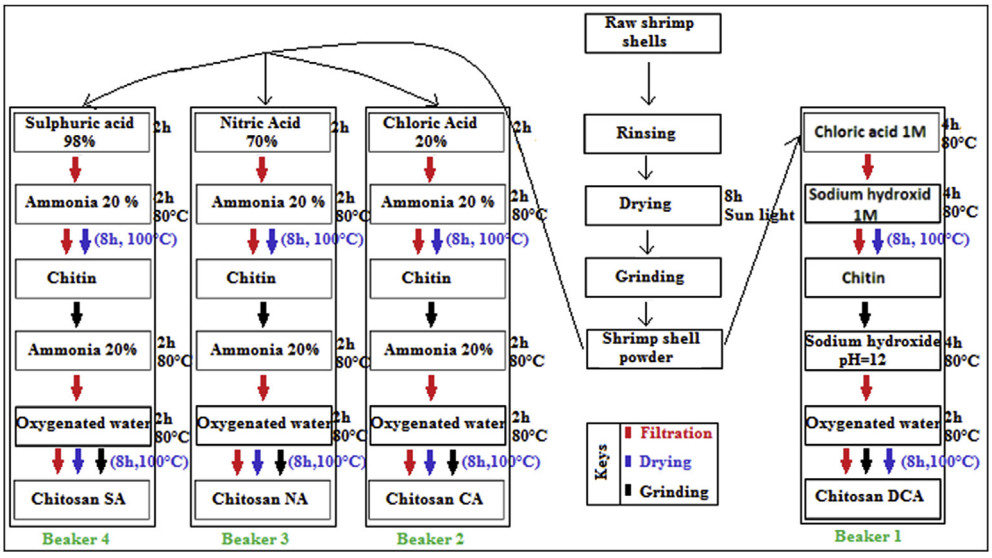

Figure 2. Experimental process of chitin and chitosan extraction.

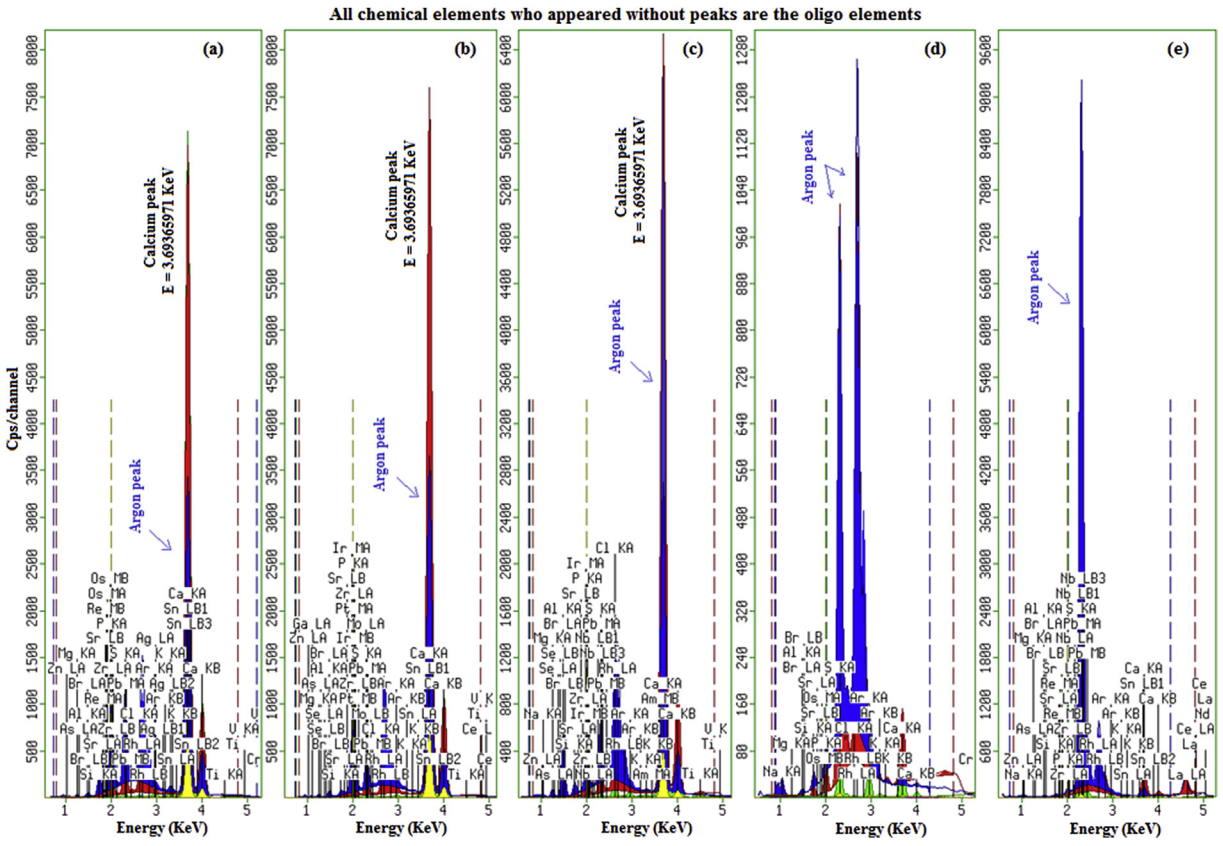

Figure 3. XRF pattern (Cps/channel Vs Energy (KeV)) of (a): Shrimp ShP, (b): Chitosan DCA, (c): Chitosan CA, (d): Chitosan NA, (e): Chitosan SA.

Table 1. Chemical elements concentrations in Shrimp ShP, Chitosan DCA, Chitosan CA, Chitosan NA, Chitosan SA.

	Samples	Shrimp ShP		Chitosan DCA		Chitosan CA		Chitosan NA		Chitosan SA	
	Compound	Conc	Unit	Conc	Unit	Conc	Unit	Conc	Unit	Conc	Unit
Major elements	MgO	1,373	%	1,344	%	0,028	%	0	ppm	920,2	ppm
	Al_2O_3	0,178	%	0,159	%	0,062	%	0,096	%	0,084	%
	SiO_2	1,549	%	0,325	%	0,972	%	0,227	%	0,177	%
	P_2O_5	5,046	%	4,439	%	0,339	%	0,337	%	0,331	%
	SO_3	0,34	%	0,102	%	0,011	%	0,079	%	0,044	%
	Cl	0,522	%	0,197	%	0,402	%	645,9	ppm	0	ppm
	K_2O	0,293	%	204,2	ppm	893,2	ppm	185,6	ppm	575,1	ppm
	CaO	41,214	%	40,824	%	0,21	%	0,24	%	1,244	%
	Fe_2O_3	0,399	%	937,9	ppm	513	ppm	45,5	ppm	131,7	ppm
	Br	0,117	%	128,5	ppm	350,9	ppm	11,1	ppm	12,8	ppm
	SrO	0,552	%	0,343	%	20	ppm	17,3	ppm	51,2	ppm
Oligo elements	TiO_2	680,1	ppm	156,4	ppm	20	ppm	0	ppm	0	ppm
	V_2O_5	18,5	ppm	13,4	ppm	7	ppm	0	ppm	0	ppm
	Cr_2O_3	30	ppm	12	ppm	5	ppm	9	ppm	0	ppm
	MnO	53,9	ppm	44	ppm	12	ppm	0	ppm	9	ppm
	CuO	126,7	ppm	45,2	ppm	95	ppm	51,7	ppm	14,8	ppm
	ZnO	175,7	ppm	90,4	ppm	0,156	ppm	0	ppm	42,5	ppm
	As_2O_3	20,2	ppm	12,7	ppm	13,3	ppm	0	ppm	2,1	ppm
	ZrO_2	1,2	ppm	0	ppm	0	ppm	0	ppm	0	ppm
	Ag_2O	817,6	ppm	0	ppm	0	ppm	0	ppm	0	ppm
	SnO_2	31,7	ppm	27	ppm	0	ppm	0	ppm	25,9	ppm
	Yb_2O_3	25,1	ppm	0	ppm	16,5	ppm	0	ppm	0,5	ppm
	PbO	8,9	ppm	0	ppm	0,366	ppm	0	ppm	2,9	ppm

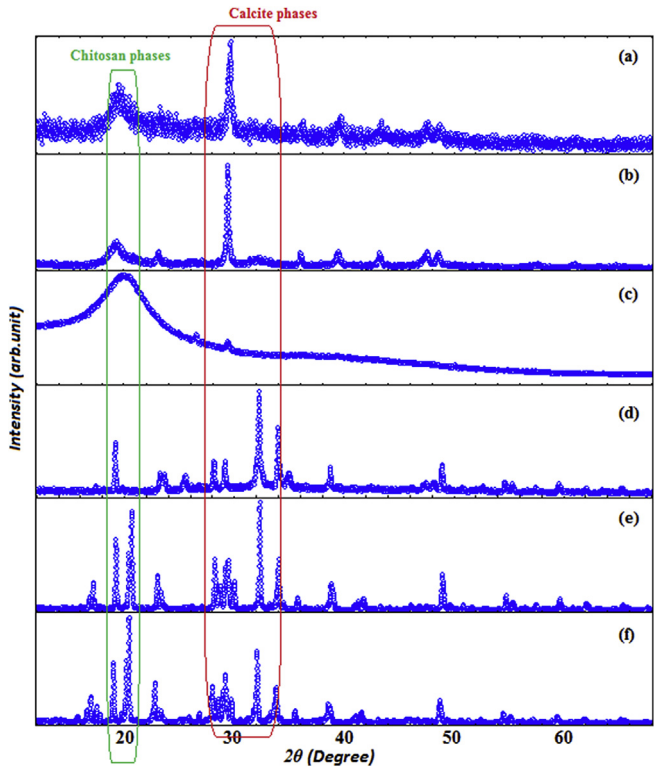

Figure 4. XRD pattern of (a): Shrimp ShP, (b): Chitosan DCA, (c): Chitosan FC, (d): Chitosan NA, (e): Chitosan SA, (f): Chitosan CA.

potential source of chitosan and must be considered. From the review of Kaur et al In 2013 [21], chitosan was extracted from waste fungal mycelium, using 0.5M of NaOH for alkali treatment at 121 °C between 30 and 45 min time duration under agitation. The acidic treatment was carried out by 0.1–0.2M of sulfuric acid under centrifugation at the same temperature and time duration of alkali treatment. The deacetylation step was performed in a basic solution with pH 8–10 by 1N of NaOH and finished by cleaning with acetone, ethanol and distilled water.

The chitosan is elicited worldwide from shrimp shells, lobsters or crabs by the classical method through generally adding acids for demineralization and bases for deproteinization then sodium hydroxide for deacetylation [16, 21]. Currently, chitin and chitosan are extracted mainly from shrimp shells, with industrial production mostly concentrated in Asia with limited production and strong global demand. The demand for chitin in 2015 was more than 60,000 T, but the world production that year was about 28,000 T. according to a report by Global Industry Analysts Inc. (chitin and chitosan derivatives market report - 2015) which shows an insufficient global production on chitin and chitosan. Global applications of the chitosan market include water treatment, food and beverages, cosmetics, bioplastics, biomedicine, agrochemicals and others. All of this previous information indicates the importance of chitin and chitosan materials. In this study, we tried to highlight the effect of a high concentration of acidity and basicity on the extraction of chitosan from shrimp shells. For this reason, we focused in this study on comparing between the effect of diluted and concentrated chloric acid. Sometimes we introduce the concentrated nitric acid and sulphuric acid for showing the effect of other acids and indicate the best acid for chitosan production. We used the diluted chloric acids 1M (usually used in chitosan production) and chloric acid 20% (CA20%), nitric acid 70% (NA70%), sulphuric acid 98% (SA98%). We employed ammonia 20% as a base for deproteinization and deacetylation in the case of concentrated acids, instead of sodium hydroxide NaOH used in case of diluted chloric acid. The first reason to use ammonia NH_4OH as a base instead of NaOH is to remove proteins in the first step and radical's acetyl group in the second, without any remains of Na^+ in chitosan product. Laribi-Habchi et al in 2015 used ammonium sulphate for chitin proteins purification [22] since ammonium sulphate is an ionic chemical compound of formula $(NH_4)_2SO_4$ with ammonium salt NH_4^+ and sulphuric acid H_2SO_4. We are looking for any changes that have occurred on chitosan in this production. All chitosan products are well characterized by different X-ray diffraction (XRD) spectroscopy, X-ray fluorescence (XRF) analysis, UV-Visible spectroscopy, Fourier Transformed Infra-Red (FTIR), Raman Spectroscopy, Thermogravimetry and Derivative thermogravimetry (TG/DTG), Scanning Electron Microscopy (SEM), Energy-dispersive X-ray spectroscopy (EDX) analysis, in order to have maximum information about the physical properties, to be referred and compared to those of commercial chitosan purchased from Fluka Chemika Company. We also studied the optical properties, absorbance, transmittance and reflectance of visible and ultraviolet light just for raw Shrimp ShP and chitosan extracted by concentrated and diluted chloric acid. We claimed the gap energy (E_g) and Urbach energy (E_u) for disorder determination. We attempt whether the concentration of acids and bases affected the degree of deacetylation (DD), the crystal structure and optical properties.

In all of this manuscript, we noted the Shrimp ShP by (Shrimp ShP), chitosan obtained by diluted chloric acid by (Chitosan DCA), chitosan obtained by concentrated chloric acid by (Chitosan CA), chitosan obtained by concentrated sulphuric acid by (Chitosan SA) and chitosan obtained by concentrated nitric acid by (Chitosan NA), commercial chitosan purchased from Fluka Chemika company by (Chitosan FC).

2. Experimental processes

2.1. Process of synthesis of chitosan DCA

To prepare chitosan DCA, we proceed by taking shrimp shells and rinsing it in water and then dry it in sunlight for 8 h. We add the chloric acid 1M and mix it for 4h at 80 °C, then rinse it again in water. The second part kicks off by adding the base of sodium hydroxide 1M following the same process (4 h mix in 80 °C). Once finished, we rinse it with distillate water and grind it. After that, we put it in the oven for 8h at 100 °C. Then, we immerse the product powder in sodium hydroxide solution (pH = 12) for 4h at 80 °C for deacetylation. The product is then ready after one last grind with porcelain mortar. We end by the whitening process with oxygenated water for 2h at 80 °C.

Table 2. Structural parameters of Shrimp ShP, Chitosan DCA, Chitosan FC, Chitosan CA, Chitosan NA and Chitosan SA.

Sample	Crystal System	Symmetry Group	Cell Parameters		2θ (°)	α = β = γ (°)
			a = b(A)	c (A)		
Shrimp ShP	Tetragonal	P 4/m m m	12.7690	6.9870	29,658	90.000
Chitosan DCA	Tetragonal	P 4/m m m	18.4464	7.0739	36,352	90.000
Chitosan FC	Tetragonal	P 4/m m m	15.4507	10.0332	20.199	90.000
Chitosan CA	Tetragonal	P 4/m m m	9.7396	25.0322	20,376	90.000
Chitosan NA	Tetragonal	P 4/m m m	18.595	4.7716	32,268	90.000
Chitosan SA	Tetragonal	P 4/m m m	18.449	5.7113	32.320	90.000

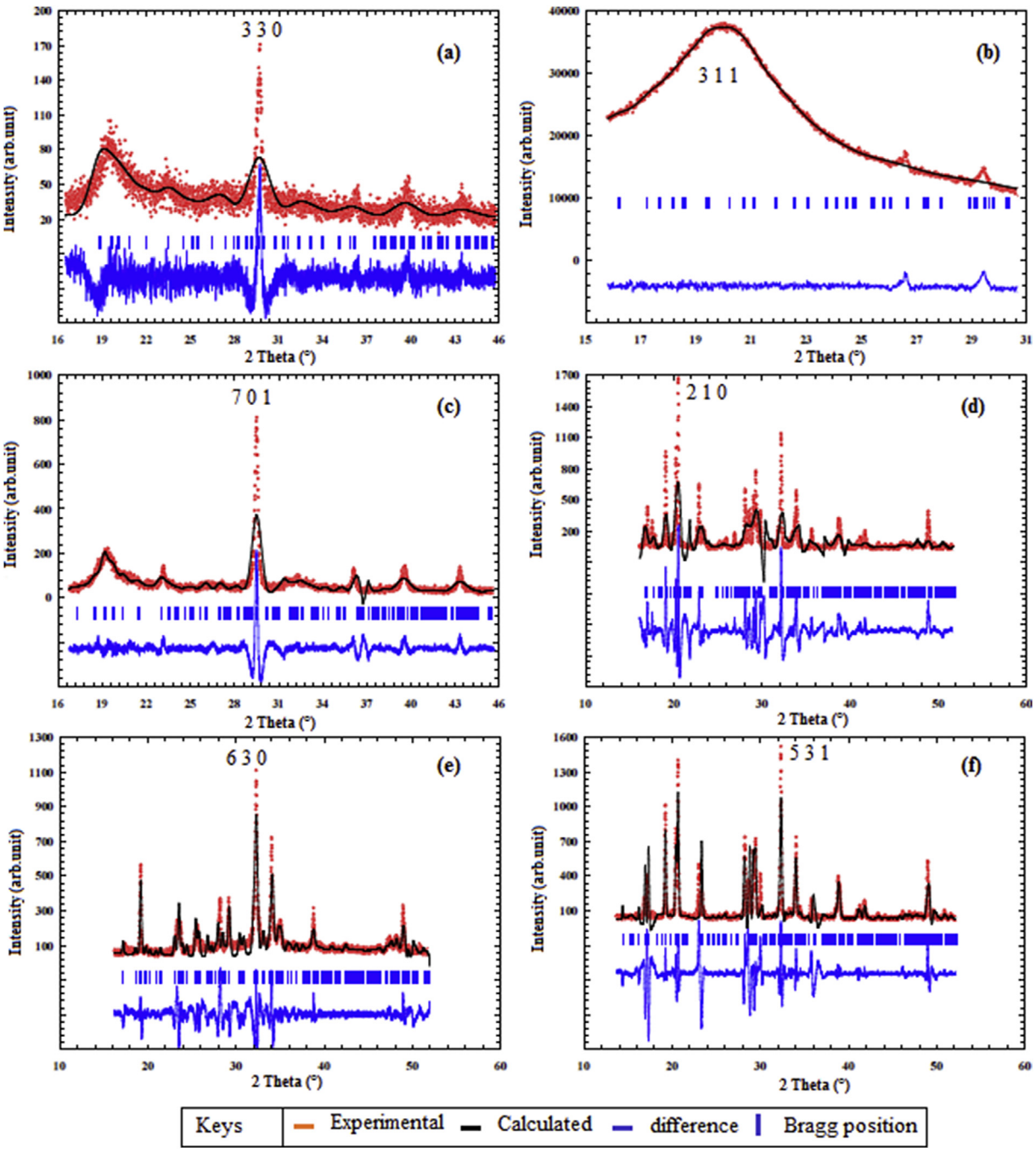

Figure 5. -XRD Reitveld refinement of (a): Shrimp ShP, (b): Chitosan FC, (c): Chitosan DCA, (d): Chitosan CA, (e): Chitosan NA, (f): Chitosan SA.

Table 3. (a): Shrimp ShP, (b): Chitosan DCA, (c): Chitosan FC, (d): Chitosan CA, (e): Chitosan NA, (f): Chitosan SA.

Sample	a	b	c	d	e	f
D (nm)	4,13	8,51	5,80	9,39	24,61	34,59

2.2. Process of synthesis of chitosan by concentrated acid and base

For the production of Chitosan CA, Chitosan NA, and Chitosan SA, we start as the process for Chitosan DCA by preparing the shell shrimps firstly by rinsing it with water, and then leave it to be dried at sunlight for 8 h. We grind the dried shrimp shells and put them separately in three 100 ml beakers, then we add in excess the chloric acid 20%, sulphuric acid 98%, nitric acid 70%, each acid in one beaker and we leave them for 2 h. The grinded shrimp shells completely dissolved in CA20%, NA70%, and SA98%. The second part begins by the separation of products from acids in three steps: filtration, well cleaning with distillate water and heat drying in order to take the filtrates in a more pure state. Then we add the ammonia 20% in drops until we get to ph = 7, and we repeat the same previous filtrations. In this case, our products are chitin. For obtaining

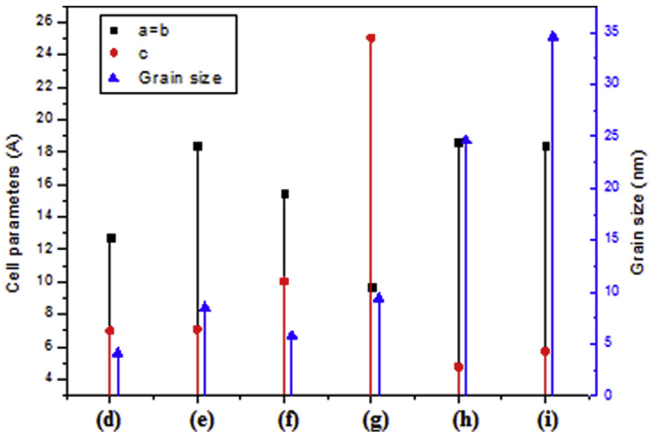

Figure 6. Grain sizes and cell parameters evolution of (d): Shrimp ShP, (e): Chitosan DCA, (f): Chitosan FC, (g): Chitosan CA, (h): Chitosan NA and (i): Chitosan SA.

the chitosan we add again in each beaker the ammonia 20% in excess and we leave them for 2 h, we do the same previous filtration to separate chitosan from ammonia. Then we wash them by hydrogen peroxide for 2 h for bleaching and drying them at 80 °C. The experimental process is summarized in Figure 2.

3. Results and discussion

3.1. X-ray fluorescence (XRF) analysis

X-ray fluorescence spectrometry (XRF) is a chemical analysis technique based on the excitation of atoms or molecules by X-Rays. These absorbed rays will be followed immediately by spontaneous secondary emission of another form of energy named fluorescence of X-Rays. The apparatus spectrometer collects all of those secondary emissions and builds the XRF spectrum were each peak corresponds to the quantitative concentration of the chemical elements within materials. This is a non-destructive analysis of the full range of elements from sodium to uranium [23]. The X-ray fluorescence spectrometer is capable of analyzing elements in concentrations from a high percentage down to ppm level. In our case, the importance of the chemical element analysis is to determine the variation of the mineral elements concentration in shrimp shells after using different acids for its demineralization in order to deduce the acids effect in its mineral part. The XRF patterns of all our products are shown in Figure 3. We will not give any consideration to blue peaks, because this appearance is due to the X-rays reflexion by argon gas used for the functioning of the apparatus. The results show the existence of oligo elements and major elements. Oligo elements in ppm (parts per million) such as Titanium Ti, Zinc Zn, Manganese Mn. We will not consider them in shrimp shells structure, because they do not occupy a major part of its structure and can also be due to background noise. Many minerals exist in raw Shrimp ShP. We note the existence of low concentration of chemical elements of magnesium Mg,

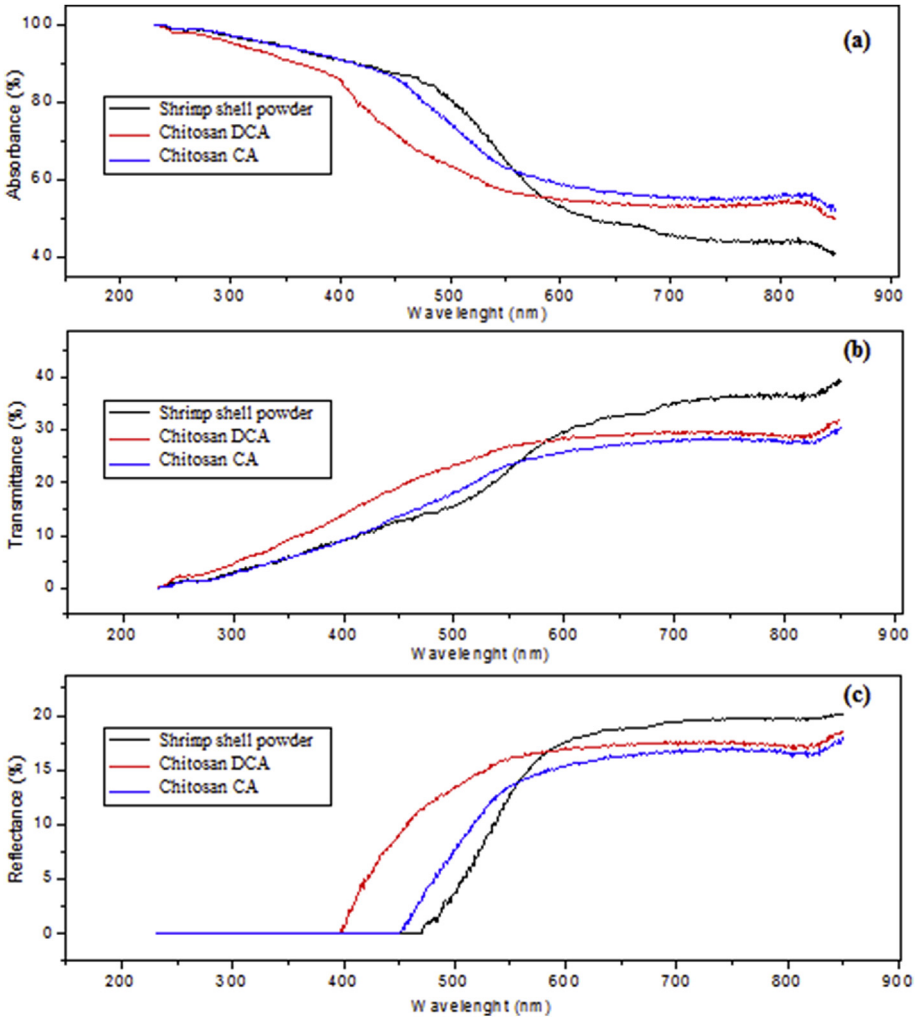

Figure 7. The Uv-Visible spectrums, (a): Absorbance, (b): Transmission (c): Reflectance of Shrimp ShP, Chitosan DCA and Chitosan CA.

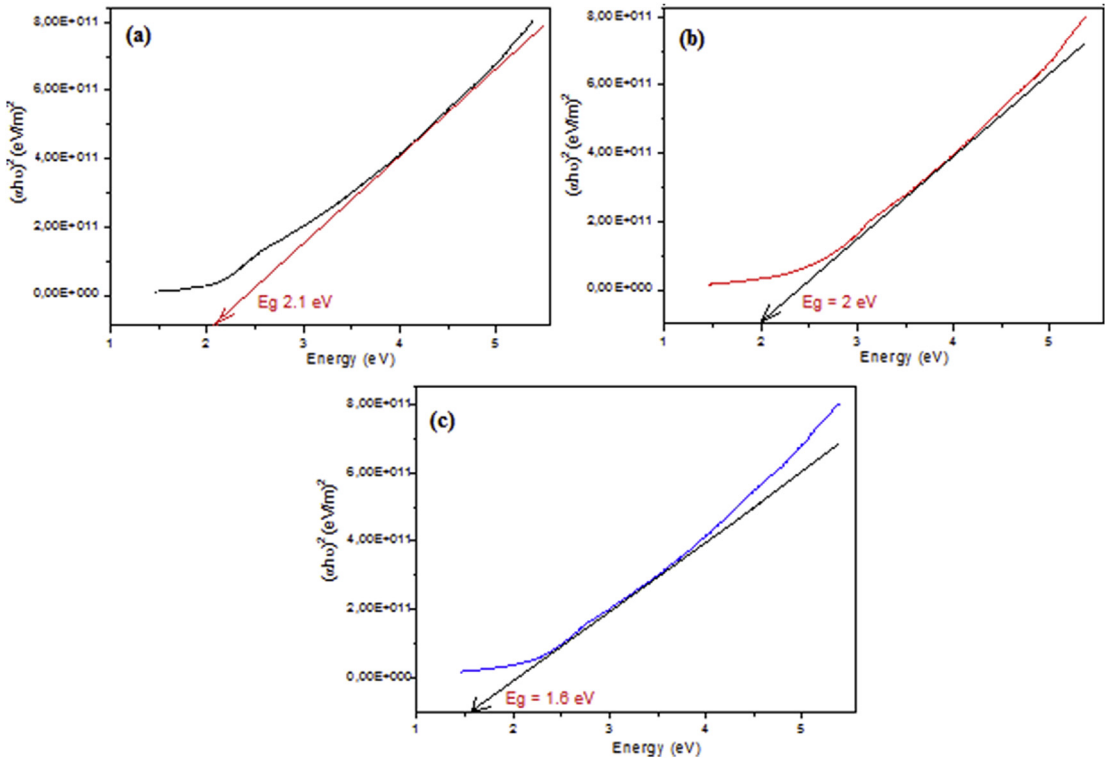

Figure 8. The determination of the optical gap energies of (a): Shrimp ShP, (b): Chitosan DCA, (c): Chitosan CA.

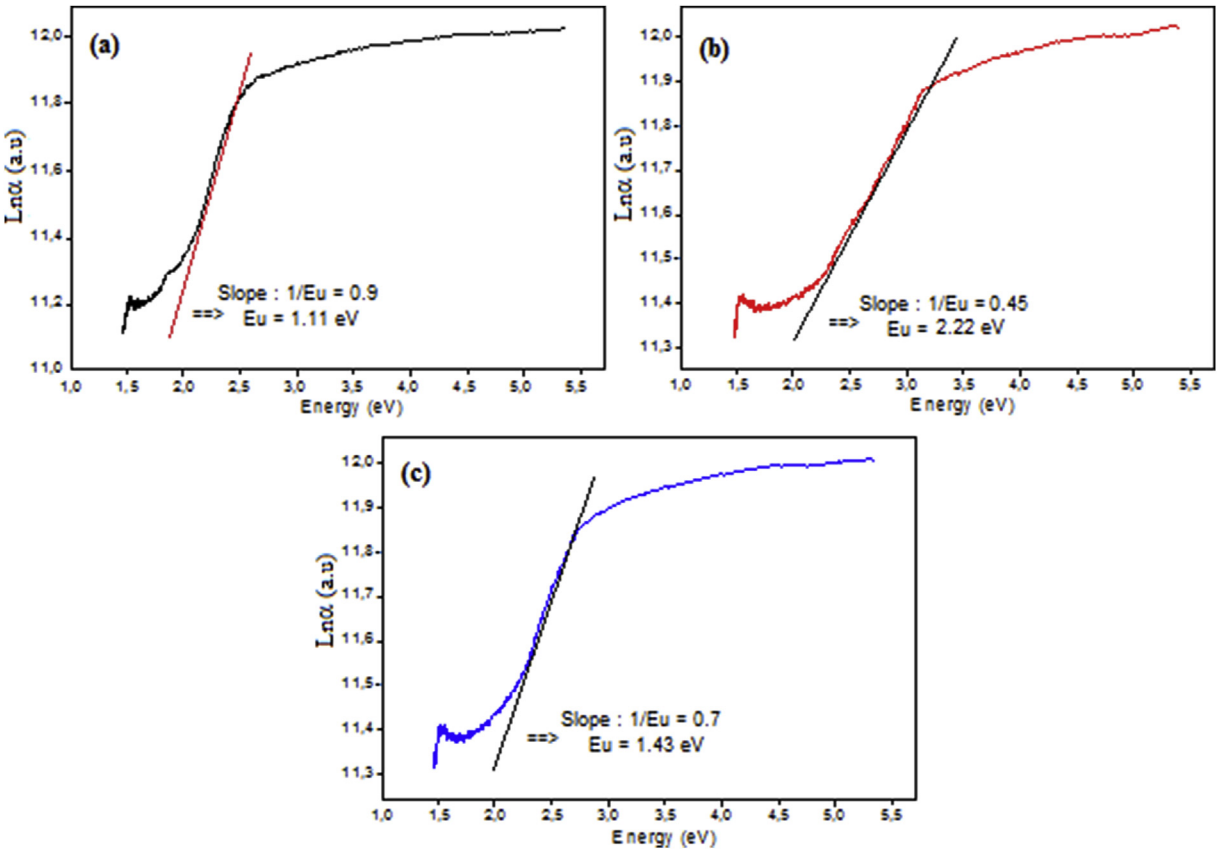

Figure 9. The determination of the optical gap energies of (a): Shrimp ShP, (b): Chitosan DCA, (c): Chitosan CA.

Table 4. Value of the gap energy and Urbach energy for the Shrimp ShP, Chitosan DCA and Chitosan CA.

Sample	Shrimp ShP	Chitosan DCA	Chitosan CA
Gap energy Eg (eV) (Err ±0.01 eV)	2.1	2	1.6
Urbach energy Eu (eV) (Err ±0.01 eV)	1.11	2.22	1.43

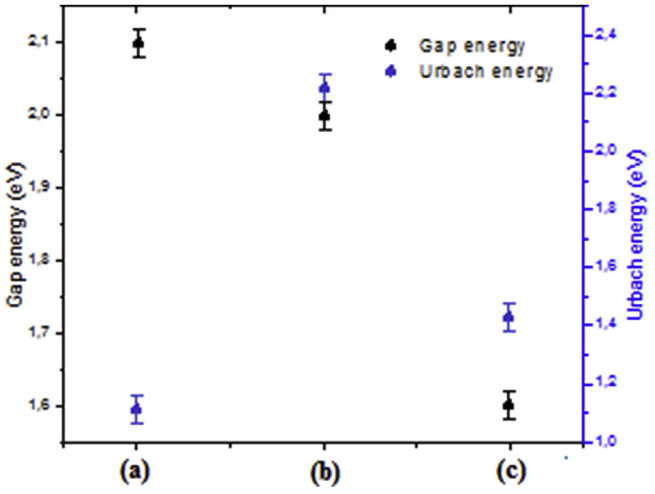

Figure 10. The representation of the optical gap energies and Urbach energies of (a): Shrimp ShP, (b): Chitosan DCA, (c): Chitosan CA.

aluminium Al, silicon Si, Potassium K, Iron Fe, and existence of Calcium Ca and phosphorus in high concentration (41.214% of CaO and 5.046% of P_2O_5). Thus, these are the essential elements that make up the shrimp shells' crystalline structure.

Each acid eliminate minerals following its effectiveness. We see the decrease of all elements' concentration in all chitosan samples, but not very much for Chitosan DCA, since its calcium oxide CaO residue is 40.824% (decrease by 0,946%). While, the CaO residues are successively 0.21% Chitosan CA (decrease by 99,49%), 0.24% for Chitosan NA (decrease by 99,417%), 1.244% for Chitosan SA (decrease by 96,988%). All chemical elements' concentrations are summarized in Table 1. We remark that carbon oxide CO and nitrogenous oxide NO which present the polysaccharides family does not appear in XRF analysis results for all chitosan samples because of secondary light interference; but we can easily deduce their concentration by the subtraction of the total concentration of appeared elements from 100% (100% - ∑%elements concentration). The (CO + NO)% concentration for Shrimp ShP, Chitosan DCA, Chitosan CA, Chitosan NA and Chitosan SA are successively 48,417%, 52,464%, 97,976%, 99,021% and 98,12 %. These results show that concentrated acids are good for chitin and chitosan extraction from

Table 5. Description of IR band of Shrimp ShP, Chitosan CA, Chitosan NA, Chitosan SA, Chitosan DCA and Chitosan FC.

Samples	IR Band cm^{-1}	Transmittance %	Description
Shrimp ShP	3315	92.74	Stretching vibration of OH and N-H group
	2200	96.33	Symmetric CH_3 stretching and asymmetric CH_2 stretching
	2175	96.68	CH stretching
	1680	95.52	($-NH_2$) amide II
	1325	95.61	*s ($-CH_3$) tertiary amide
	1175	93.80	Stretching vibration of PO_4^{3-}
	1000	94.81	*as(C-O-C) and *s(C-O-C)
	700	93.15	NH out – of – plane bending
	670	91.20	OH out – of – plane bending
Chitosan CA	3391,88	81,23	Stretching vibration of OH and N-H group
	1407,54	58,21	Angular deformation of CH2
	1114,38	67,49	C-C and C-O stretching
	874,50	78,55	Antisymmetric stretching of the CO_3^{2-} ion
	514,05	43,97	Vibration of cis C-H
Chitosan NA	2898.73	86,00	CH stretching modes
	1640.72	87,28	Stretching vibration C=O
	1425.67	61,53	Angular deformation of CH_2
	1109.09	62,33	C-C and C-O stretching
	513.90	57,45	Vibration of cis C-H
Chitosan SA	1686.58	100,00	Stretching vibration C=O
	1340.88	87,66	Angular deformation of CH_2
	1110.45	8,39	C-C and C-O stretching
	876.63	92,34	Antisymmetric stretching of the CO_3^{2-} ion
	615.50	76,31	Vibration of cis C-H
Chitosan DCA	1413.15	93,03	Angular deformation of CH_2
	1025.67	10,52	C-C and C-O stretching
	873.14	12,31	Antisymmetric stretching of the CO_3^{2-} ion
	564.13	100	Ibration of cis C-H
Chitosan FC	3300,00	100	Stretching vibration of OH and N-H group
	1640.72	87,28	Stretching vibration C=O
	1425.67	61,53	Angular deformation of CH_2
	1035,86	99,90	C-C and C-O stretching
	513.90	57,45	Vibration of cis C-H

* = stretching vibration, $*_s$ = symmetric stretching vibration and $*_{as}$ = asymmetric stretching vibration.

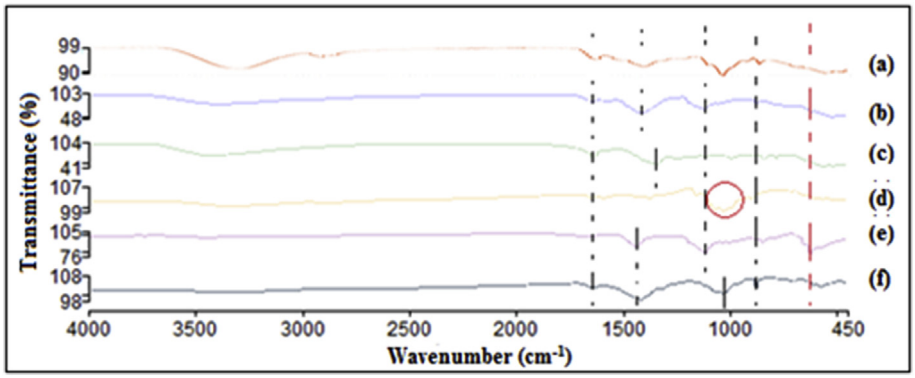

Figure 11. The FTIR spectrums of (a): Shrimp ShP (b): Chitosan CA, (c) Chitosan NA, (d): Chitosan FC, (e): Chitosan SA and (f): Chitosan DCA.

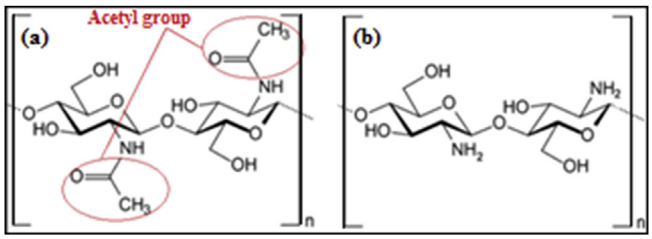

Figure 12. Chemical formula of (a): Chitin and (b): Chitosan.

shrimp shells, due to their higher potential to remove minerals [24]. Therefore, the carbon C, nitrogenous N and oxygen O has been the essential components of our samples. We cannot directly conclude that our products are chitosan or chitin due to their similar components, but we can do it by the degree of deacetylation DD [25, 26] (we further discuss it below in FTIR analysis paragraphs). The border between chitosan and chitin corresponds to a DD of 50 %: Above this value, the compound is called chitosan, if not, the compound is chitin. And the role of the second use of the base is to remove acetyls group from chitin in order to be chitosan.

3.2. X-ray diffraction (XRD) analysis

The crystallinity of samples was evaluated by wide angle X-ray diffraction analysis using a Bruker D8 ADVANCE Powder XRD apparatus. Common targets used in X-ray tubes include Cu and Mo, that emit respectively 8 keV and 14 keV X-Ray energies with corresponding wavelengths of 1.54 Å and 0.8 Å. This diffractometer functioned by Cu Kα radiation. The XRD pattern obtained for Shrimp ShP, Chitosan DCA, Chitosan CA, Chitosan NA, Chitosan SA, and Chitosan FC are shown in Figure 4 followed by their Rietveld refinement, aim to deduce the structural parameters of all chitosan samples. The major peaks for all samples extracted by concentrated acids are similar to this of Chitosan FC with a difference in the degree of crystallinity [27] appeared in the diffraction angle near to $2\theta = 20^{\circ}$ that is the characteristic region of chitosan phases, and near to $2\theta = 30^{\circ}$ for Shrimp ShP and Chitosan DCA, that is the characteristic region of calcite and calcium phosphate family. These primary results show that the use of diluted acid is not the favorite way to extracted chitosan from shrimp shells. It is incapable to remove all minerals from shrimp shells (unlike concentrated acid). The XRD patterns shows the small structural change between shrimp shells and Chitosan DCA, and more structural changes between shrimp shells and chitosan extracted by concentrated acids and Chitosan FC. These changes are due to the mineral removal effectiveness of each acid. In addition, the calcium and phosphorus are the mains minerals components in shrimp shells. The elimination of calcite is not easy by diluted acid, also the presence of calcium and phosphorus in the same time in the aqueous media leads to the formation of hydroxyapatite crystallite, can't be removed or solved by the diluted acid. For these two reasons, demonstrate that the diluted acids have a small effect and the concentrated acids have a high effect on shrimp shells structure due to easiness removal of calcium and phosphorus mostly for nitric acid that can solve the hydroxyapatite. Therefore, what's affect bases on shrimp shells crystal structure? Shrimp shells contain proteins as organic part, and it's known that those primary structures, corresponds to the linear succession of the amino acids without reference to their spatial configuration. Thence, proteins are the amino acid polymers, linked together by peptide bonds. The role of the bases is to remove them from shrimp shells, but it does slightly affect its crystallization because these proteins do not form their structure.

In a view to define the structural parameter variations related to the use of some acid or other, we performed the Rietveld refinement by FullProf software. The structural results are summarized in Table 2, and the FullProf graphs are shown in Figure 5. These graphs show a good Reitveld refinement for all samples, because the calculated pattern and the experimental pattern are almost congruous, with a small difference between them. The major mineral part of shrimp shells crystallizes in tetragonal system with (P 4/m m m) symmetry groups and the same for all chitosan samples that they save these properties after extraction. We remark an increase in cell parameters of all chitosan samples comparing to those of Shrimp ShP due to the decrease of minerals' concentration that lead to a decrease of number of ionic bonds.

The XRD patterns indicate that the chitosan contain also an amorphous form due to the presence of OH and NH_2 groups which form the intermolecular hydrogen's bond. Thus, this distribution will have some regularity to build easily the crystalline regions. Similarly to the results reported in the preparation and characterization of the chitosan binary blend [28]. The Debye-Scherrer method was used to obtain the grains' size from X-ray diffraction measurements by following relationship (1) [29]:

$$D = \frac{k.\lambda}{B.\cos(\theta)} \quad (1)$$

Table 6. DA and DD of Chitosan CA, Chitosan NA, Chitosan SA, Chitosan DCA and Chitosan FC.

Samples	DA%	DD%
Chitosan CA	19,25187901	80,748121
Chitosan NA	19,26173236	80,7382676
Chitosan SA	19,25187901	80,748121
Chitosan DCA	19,14694703	80,853053
Chitosan FC	24,55902372	75,4409763

Where D is the grin's size diameter, B is the broadening of the diffraction line measured at half-maximum intensity, λ is the wavelength of (Cu Kα), h is the Bragg angle for a given diffraction and k is a constant, in general equal to 0.9 for powders. The grain sizes results are shown in Table 3.

We remark an increase in the grain sizes between Shrimp ShP and all our chitosan due to an increase in structural parameters. See Figure 6.

3.3. Optical and opto electronic properties

We want to explore the variance in opto-electronic behavior between Shrimp ShP and two types of chitosan. One extracted by diluted acid and the second extracted by concentrated acids. For this objective, we choose Chitosan DCA and Chitosan CA. The Uv-visible spectroscopy analysis was carried out using a T92 + UV-visible spectrophotometer.

Figure 7 show the optical spectrums of absorbance, transmittance and reflectance as function to the wavelength in the Uv-visible range between 200 and 800 nm. The spectrums indicate that all samples have a high absorption of ultraviolet lights around 90–99% in the wavelength range of 200–400 nm with very a low transmission in the absence of reflexion. As well, we remark a darkness between 600 and 800 nm since to the good light absorption by samples circa 45% for Shrimp ShP and and 54% for Chitosan DCA and 57% for Chitosan CA, and transmission nearly 36% for Shrimp ShP and 29% for Chitosan DCA, and 28% for Chitosan CA, and reflexion about 19% for Shrimp ShP and 17% for Chitosan DCA, and 15% for Chitosan CA. This incongruity is due to the elimination of minerals and acetyl groups. The samples' absorbance above are very important allows us to calculate the coefficient of absorption α which was obtained by dividing the absorbance of each sample by its thickness.

As it is shown in Figure 8, the optical gap energy E_g was determined from the absorption coefficient α by the relationship (2) [30-31]. Thus, the E_g is obtained by intersection of the tangent of the linear part of the curve of $(\alpha h\nu)^2 = f(h\nu)$ with the abscissa axis represents the energy hν.

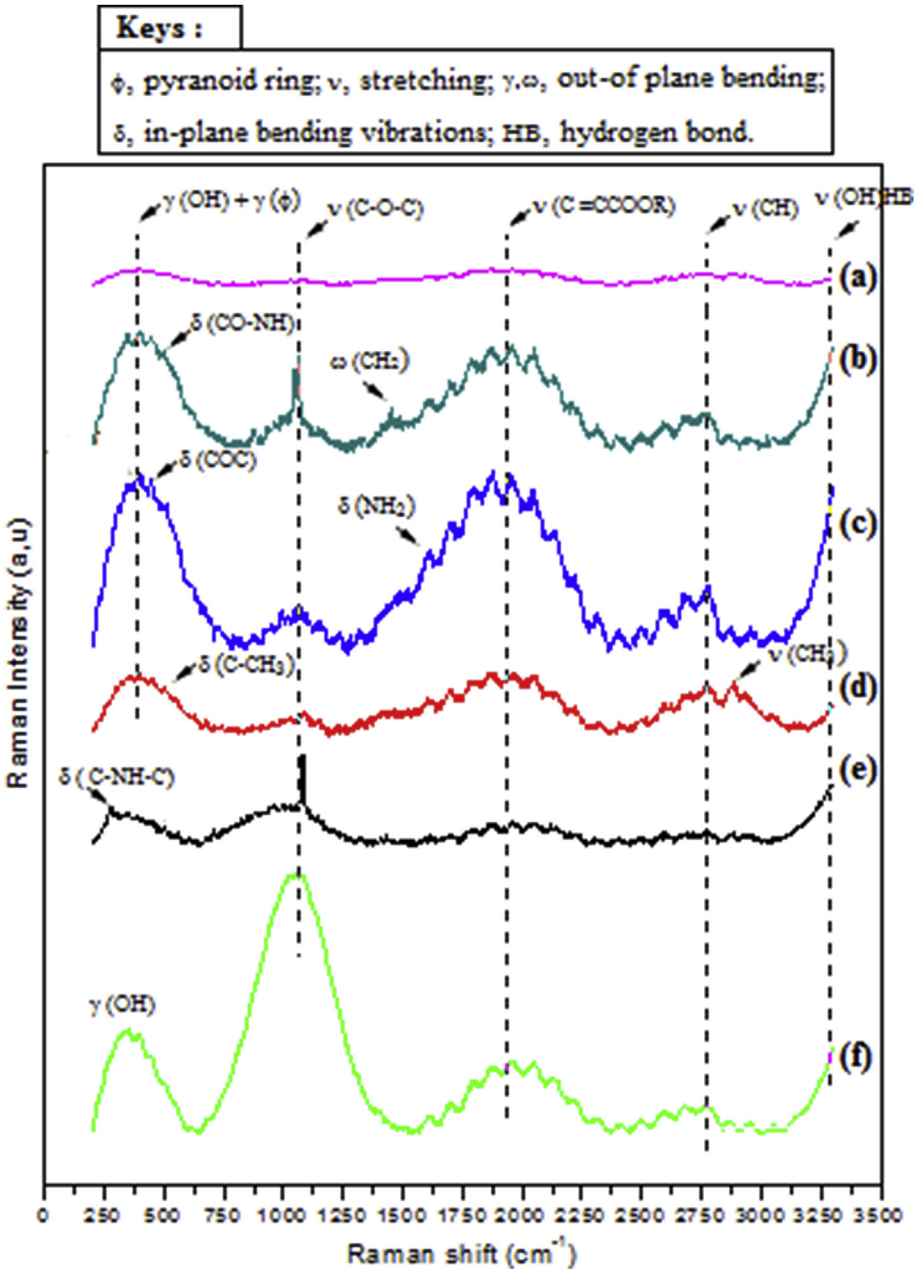

Figure 13. Raman spectrums of (a): Chitosan FC, (b): Chitosan SA, (c): Chitosan NA, (d): Chitosan CA, (e): Chitosan DCA, (f): Shrimp ShP.

Table 7. Raman vibration modes depending to wavenumber for Shrimp ShP, Chitosan DCA, Chitosan FC, Chitosan CA, Chitosan NA and Chitosan SA.

Keys: φ, pyranoid ring; ν, stretching; δ, in-plane bending vibrations; γ,ω, out-of plane bending; HB, hydrogen bond.

Shrimp ShP		Chitosan DCA		Chitosan FC	
Wavenumber (cm^{-1})	Assignments	Wavenumber (cm^{-1})	Assignments	Wavenumber (cm^{-1})	Assignments
268 277	δ(C-NH-C)+γ(OH)	276	δ(C-NH-C)+γ(OH)	269 277 301	δ(C-NH-C)+γ(OH)
352 376 396 439 446	γ(OH) + γ(φ)	360 369 382 390 402 420 432 444	γ(OH) + γ(φ)	349 388 398 412 449	γ(OH) + γ(φ)
897	ν(φ)+ρ(CH_2)	465	ν(φ)+ρ(CH_2)	470	δ(COC)
943	ν(CN)	899	ν(φ)+ρ(CH_2)	557	ν(NH)+γ(C=O)+ω(CH_3)
993	ν(φ)+δ(CH)	928	ν(CN)	702	ω(NH_2)+δ(φ)
1102	ν(C-O-C)+ν(φ)+ν(C-OH)+ ν(C-CH_2)+δ(CH)+ρ(CH_2)+ ρ(CH_3)	991	ν(φ)+δ(CH)	944	ν(CN)
1269	δ(OH...O)+ν(C-C)+ν(C-O)+ δ(CH)+ρ(CH_2)	1041	ρ(CH_3)+δ(CH)+ δ(OH)	1140	ν(C-O-C)+ν(φ)+ν(C-OH)+ ν(C-CH_2)+δ(CH)+ρ(CH_2)+ ρ(CH_3)
1409	δ(CH_3)+δ(CH)	1080 1107 1117 1142	ν(C-O-C)+ν(φ)+ν(C-OH)+ ν(C-CH_2)+δ(CH)+ρ(CH_2)+ ρ(CH_3)	1255	δ(OH...O)+ν(C-C)+ν(C-O)+ δ(CH)+ρ(CH_2)
1607	δ(NH_2)	3257	ν(OH)HB	1322	ν(CN)+δ(CH)
2760	ν(CH)			1376	δ(CH_2)+δ(CH)+δ(OH)+ν(φ)
3284	ν(OH)HB			1407	δ(CH_3)+δ(CH)
				1454	δ(CH)+ω(CH_2)+δ(OH)
				1593	δ(NH_2)
				2809	ν(CH_3)
				2883	ν(CH_2)
				2883	ν(CH_2)
Chitosan CA		**Chitosan NA**		**Chitosan SA**	
Wavenumber (cm^{-1})	**Assignments**	**Wavenumber (cm^{-1})**	**Assignments**	**Wavenumber (cm^{-1})**	**Assignments**
269 277	δ(C-NH-C)+γ(OH)	353 364 387 395 403 414 425 441	γ(OH) + γ(φ)	269	δ(C-NH-C)+γ(OH)
363 369 388 398 411 444	γ(OH) + γ(φ)	496	δ(CO-NH)+δ(C-CH_3)+ δ(COC)	352 376 385 398 420 427 443	γ(OH) + γ(φ)
484	δ(CO-NH)+δ(C-CH_3)+ δ(COC)	567	ν(NH)+γ(C=O)+ω(CH_3)	478	δ(COC)
564	ν(NH)+γ(C=O)+ω(CH_3)	1457	δ(CH)+ω(CH_2)+δ(OH)	497	δ(CO-NH)+δ(C-CH_3)+ δ(COC)
1030	ρ(CH_3)+δ(CH)+ δ(OH)	1661	ν(CO)	568	ν(NH)+γ(C=O)+ω(CH_3)
1092 1102 1109	ν(C-O-C)+ν(φ)+ν(C-OH)+ ν(C-CH_2)+δ(CH)+ρ(CH_2)+ ρ(CH_3)	2735	ν(CH)	991	ν(φ)+δ(CH)
1381	δ(CH_2)+δ(CH)+δ(OH)+ν(φ)	3217	ν(OH)HB	1046	ρ(CH_3)+δ(CH)+ δ(OH)
1407	δ(CH_3)+δ(CH)			1093	ν(C-O-C)+ν(φ)+ν(C-OH)+ ν(C-CH_2)+δ(CH)+ρ(CH_2)+ ρ(CH_3)
1454	δ(CH)+ω(CH_2)+δ(OH)			1450	δ(CH)+ω(CH_2)+δ(OH)
1585	δ(NH_2)			1587	δ(NH_2)
1657	ν(CO)			1657	ν(CO)
2737	ν(CH)			2741	ν(CH)
2822	ν(CH_3)			3229	ν(OH)HB
2883	ν(CH_2)				
2931	ν(CH_3)				
3291	ν(OH)HB				

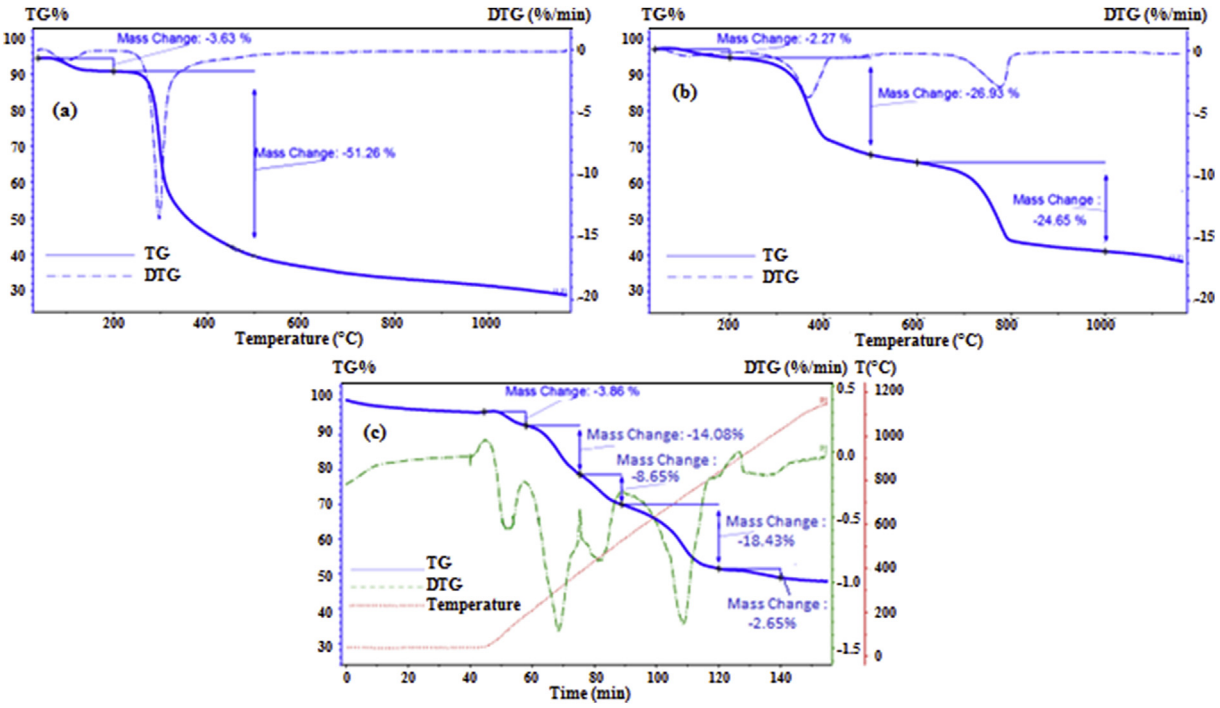

Figure 14. Thermogravimetry TG and Derivative thermogravimetry DTG for (a): Chitosan FC, (b): Chitosan DCA and (c): Chitosan CA.

$$\alpha h\nu = \alpha_0 \cdot \left(h\nu - E_g\right)^n \quad (2)$$

Where: α_0 is a constant and sometimes called the band tailing parameter, it is an energy independent and constant Eg is the gap energy, which is the forbidden zone between the valence band below the Fermi level and conduction band above the Fermi level according to the density of states model, proposed by Mott and Davis [32, 33], n is the power factor of the transition mode equal to 0.5 in our case for the materials that have a direct gap.

The Urbach energies E_u (Called also the disorder) were deduced from the reciprocal slope of the linear part of the curve of $Ln(\alpha) = f(h\nu)$ by the Urbach relationship (3). See Figure 9.

$$Ln(\alpha) = Ln(\alpha_0) + \frac{h\nu}{E_u} \quad (3)$$

The results show a decrease in the gap energy 2.1 eV for Shrimp ShP, 2 eV for Chitosan DCA and 1.6 eV for Chitosan CA. This decrease is due to the elimination of proteins and all impurities. While, the Chitosan CA is more conductor than Chitosan DCA and Shrimp ShP, thanks to its small gap energy. These products can be candidate to be used in bio-semiconductor, and do not have any danger for environment or health. The Urbach energy is the electronic disorder in crystal. We remark that the Urbach energy is lower for Shrimp ShP with value equal to 1.11 eV, this energy increase for Chitosan DCA with value equal to 2.22 eV and for Chitosan CA with value 1.43 eV. These variations depend to the disorder or delocalized states of each sample. After demineralization, and deproteinization, the numbers of defects in structure increase leading to an increase in the electronic disorder for the Chitosan DCA and Chitosan CA which exhibit the increase their Urbach energies value. Consequently, the Shrimp ShP has a low number of defects. The values of the E_g and E_u were summarized in Table 4 and represented in Figure 10.

3.4. Fourier Transformed Infra-Red (FTIR) spectral analysis

The infrared spectrum is obtained by using an infrared spectrophotometer (Perkin Elmer spectrum version 10.4.2). The system is considered well-defined wavelength that can be passed through the sample who being studied. The abscissa axis represents the wavenumbers expressed in (cm^{-1}) equal to the inverse of the wavelength. The magnitude is progressively modified when recording of spectrum and expressed as a percentage (%) in the ordinate axis representing the transmittance (T %). In the absence of all absorptions, the baseline is continuous with a transmittance of 100%. On the other hand, if the sample absorbs an incident beam the vibration of the bonds will altered in the molecules, and the absorption band with a peak pointing downwards appears in the spectrum in the range 400–4000 cm^{-1}. There are several types of vibration, for example: The longitudinal vibration of the bonds where the distance between two atoms varied, and the angular deformation where the nail between the bonds varied. The infrared spectrum provides information concerning the nature of the bonds existed in the material and therefore on its characteristic groups. The FTIR spectrum of the Shrimp ShP showed seven major peaks corresponding to the following wavenumbers 670, 700, 1000, 1175, 1420, 1325 and 1680 cm $^{-1}$ as shown in Figure 11(a) and their bands' descriptions are shown in Table 5. The FTIR analysis showed a specific band appears near to 1320 cm^{-1} for N-acetylglucosamine, and it is often used as the reference band for chitin and chitosan. The amide II band are shown in well-defined peak in 1680 cm^{-1}. The characteristics band of the -OH, $-NH_2$, -CO groups were appeared respectively in 670, 700, 1000 cm^{-1}, and they are chosen for the calculation of the extent of N-acetylation [34]. The strips in 2170–2200 cm^{-1} correspond to the stretch band of the CH groups. The FT-IR peaks in 690, 700, 1000, 1325, 1680, 2175 and 2200 cm^{-1} are similar to those of chitosans' peaks as shown in Figure 11 where we remark a great similarity between FTIR spectrums of the all chitosan samples obtained in this work and the Chitosan FC, which we regrouped all their functional groups a in Table 5. Besides, we notice that the bands corresponding to the inorganic carbonates are likewise to those of Shrimp ShP, located in 1425 and 874 cm^{-1} even if there is a displacement of the peaks depending on the acid used in the extraction of the chitosan. The peaks in 1175 cm^{-1} corresponding to the stretching vibration of PO_4^{3-} in Shrimp ShP are lost in all chitosans after performing the demineralization. The deproteinization is evidenced by the decrease in the signal intensity and changes in the regions of the CH stretching modes and the angular deformation of the CH_2 groups existing in the proteins. The

main signals observed for stretching of C=O band is in 1640.72 cm^{-1}. In addition, the bands located between 1000 and 1150 cm^{-1} is mainly corresponding to the stretching ring of CC and CO groups. Else, the wide bands above 3000 cm^{-1} are related to the overlap of the stretching vibration of the OH and NH bonds [35, 36].

On the other hand, the characterization of the chitosan requires the determination of its degree of deacetylation (DD) that is calculated by relationship (5). The degree of deacetylation (DD) of chitosan is more than 50%. FTIR spectroscopy is a rapid technique for qualitatively evaluating the degree of acetylation (DA) from the relationship (4) [15-16] by calculating the absorbance ratios of a characteristic band of an acetyl group on a band common to acetylated and deacetylated units. In a chemical composition of chitin, being the acetyl group with a chemical formula: C_2H_3O and a molar mass: 43.05 g mol^{-1}. But it is not the same for chitosan whose the acetyl group have been previously eliminated by the base. See Figure 12. The DA and DD are reported in Table 6.

$$DA\% = 31.92.\left(\frac{A_{1320}}{A_{1420}}\right) - 12.20 \quad (4)$$

$$DD\% = 100\% - DA\% \quad (5)$$

Where A_{1320} and A_{1420} are respectively the absorbance in 1320 and 1420 cm^{-1}. The peak in 1320 cm^{-1} correspond to the characteristic band of amide group (-OH, $-NH_2$, -CO).

The degree of deacetylation increase owing to decrease of the number of the acetyl groups due to the protonation of the $-NH_2$ function on the C-2 position of the repeating unit D-glucosamine, offering chitosan with a high quality.

3.5. Raman Spectroscopy analysis

Raman Spectroscopy is a non-destructive analysis that provides information about chemical properties and vibrational modes of the molecules. It provides too several information about structure, phase, crystallinity of materials. This technique is based to the excitation of the chemical bonds inside material by laser light in the range of wavenumber typically between 250 and 3500 cm^{-1}. Each chemical bond provides the most assignment response if it is excited by its resonance energy. Generally, this technique is used to determine the vibrational modes of molecules such as pyranoid ring, in-plane or out-plane bending and the stretching vibrations. The Raman spectroscopy analysis for all our chitosan samples was carried out using DRX2 Raman Microscope apparatus. All Raman spectrums are exposed in Figure 13. As can be seen in figure, all essential characteristic peaks of chitosan assignments appeared in each spectrum [28, 29, 30, 31, 32, 33, 34, 35, 36, 37, 38]. Whereas the peaks in 470, 1000, 1800, 2630, 3250 cm^{-1} correspond respectively to the stretching vibration of (C-C(=O)-C), the stretching vibration of (C-H), the in-plane bending vibrations of (C=CCOOR) and (C=O), the in-plane bending vibrations of (CH) rings, the stretching vibration of (NH_2). The stretching vibrations in 1000 cm^{-1} and 1800 cm^{-1} are mainly the special peaks of chitosan [39]. We compared our results with those of the literature [40, 41], they are congruent. Besides, the Raman analysis results confirm the molecular vibration modes observed in our chitosan samples by FTIR analysis. Moreover, other vibrational modes of low wavenumber frequencies were appeared in Raman spectrums (did not appear in FTIR spectroscopy), some modes are noted in Figure 13 and the majority are regrouped in Table 7. Our results are congruent to the study of A.ZAJAC et al [42].

Furthermore, the effect of diluted or concentrated acids on Shrimp ShP on its crystallinity is more visible by Raman spectroscopy following the shape and intensity of peaks. We note that Shrimp ShP is more crystalline than all our chitosan samples because its build slowly with the growth of shrimp without composition disequilibria or abnormal condition. The crystallinity of the chitosan was affected by its extraction method, especially by acid used. Relying on spectrums intensities, we classify the crystallinity of our chitosan samples in this descending sequence: Chitosan NA, Chitosan SA, Chitosan CA, Chitosan DCA, and Chitosan FC. Because the concentrated acids clean samples from any impurity, which give chitosan more opportunities for recrystallization after washing with distilled water and air drying.

3.6. Thermogravimetry TG and derivative thermogravimetry DTG

Thermogravimetric analysis TGA is a thermal analysis that consists of measuring the mass variation of sample in terms of time, through a determined and controlled range of the temperature, with good accuracy of the three measurements: mass, time and temperature. The resulting curve (mass m vs temperature T) provides information about the composition and thermal stability of material [43]. This measurement is often used in research to determine the characteristics of materials with a view to estimate its kinetics of oxidation at high temperature. Equally to determinate of the temperatures of degradation, the percentage of organic and inorganic parts in material compounds. It can provide other several information on physical phenomena, such as phase transitions, absorption, desorption and thermal decomposition. The Derivative thermogravimetry DTG is the difference thermogravimetry ratio of measurement of weight loss at heating. From the DTG curves, we can determine the number of thermal events to which the substance has been subjected, because each DTG peak, at any temperature gives the rate of mass loss (dm/dT in mg/min) within its temperature range [T_i-T_{max}-T_f], where T_i, is the temperature of first mass loss, T_f is the temperature of final mass loss and T_{max} is the temperature of the maximum mass loss rate. In 1954, Paulik – Erdey developed the first thermobalance able to record TG and DTG curves at the same time [44].

Thermogravimetric analysis (TG-DTG) were performed by NETZSCH STA 449F3 Thermogravimeter apparatus, using arbitrarily 24.8 mg of Chitosan FC, 28.8 mg of Chitosan DCA and 31.9 mg of Chitosan CA with heating ratio of 10 °C/min in nitrogen atmosphere with 20.0 mL/min as flow rate of protective gas and 70.0 mL/min as flow rate of purge gas in sample port of platinum until temperature range of 1200 °C. The TG and DTG curves for Chitosan FC, Chitosan DCA and Chitosan CA are shown in Figure 14. The Chitosan FC displays two stages of thermal degradation. The first stage of thermal decomposition started from 62 °C to 145 °C. The peak at the DTG at 100 °C showed an initial mass loss of 3.63 %, referring to the physically adsorbed water surface of the polymer. The second stage of mass loss is subdivided in two parts, the first part for rapid mass loss 51.26 % between 226 and 500 °C with maximum peak of 297 °C in the DTG curve and the second part for slow mass loss 6.35 % between 500 and 813 °C without any range of mass stabilization, referring to the decomposition of the polysaccharide structure. The Chitosan DCA undergoes three stages of mass loss. The first stage starting from 75 °C to 150 °C with a maximum peak at 114 °C showed an initial mass loss of 2.27 %, due to release of water in surface and inside polymer. The second step of mass loss 26.93 % is in the range of temperature from 196 to 516 °C with maximum peak of 367 °C according to the first degradation of polymeric carbohydrate molecules whish are consisting of carbon (C), hydrogen (H) and oxygen (O) atoms. The third round of mass loss by 24.65 % with maximum peak of 775 °C between 606 and 1001 °C, after crystal structure destruction and liberation of the last polysaccharide composed of randomly distributed β-(1→4)-linked D-glucosamine (deacetylated unit) and N-acetyl-D-glucosamine (acetylated unit).

Chitosan CA had five parts of thermal degradation on account of his composition and crystalline structure. The first mass loss by 3.86 % from 40 °C to 170 °C with DTG maximum peak at 110 °C, due to water clearance. Then from 184 to 385 °C with DTG maximum peak at 304 °C and mass loss by 14.08 %. The next round of mass loss is by 8.65 % between 390 and 530 °C with maximum peak of 450 °C, due to polysaccharides decomposition. Afterward, the mass decrease by 18.43 % between 530 and 840 °C with DTG maximum peak at 724 °C due to degradation of polymeric carbohydrate after crystal structure

Table 8. - Thermal events observed in Chitosan FC, Chitosan DCA and Chitosan CA in the TG and DTG curves

Range	Thermal events	Samples		
		Chitosan FC	Chitosan DCA	Chitosan CA
1°	Temperature range T_i-T_f (°C)	62–145	75–150	40–170
	DTG T_{max} (°C)	100	114	110
	Mass loss (%)	3.63	2.27	3.86
2°	Temperature range T_i-T_f (°C)	226–500	196–516	184–385
	DTG T_{max}	297	367	304
	Mass loss (%)	51.26	26.93	14.08
3°	Temperature range T_i-T_f (°C)	500–813	606–1001	390–530
	DTG T_{max}	–	775	450
	Mass loss (%)	6.35	24.65	8.65
4°	Temperature range T_i-T_f (°C)	–	–	530–840
	DTG T_{max}	–	–	724
	Mass loss (%)	–	–	18.43
5°	Temperature range T_i-T_f (°C)	–	–	840–1030
	DTG T_{max}	–	–	1000
	Mass loss (%)	–	–	2.65

Table Keys: T_i: Initial temperature, T_f: Final temperature, T_{max}: Temperature of the maximum mass loss rate

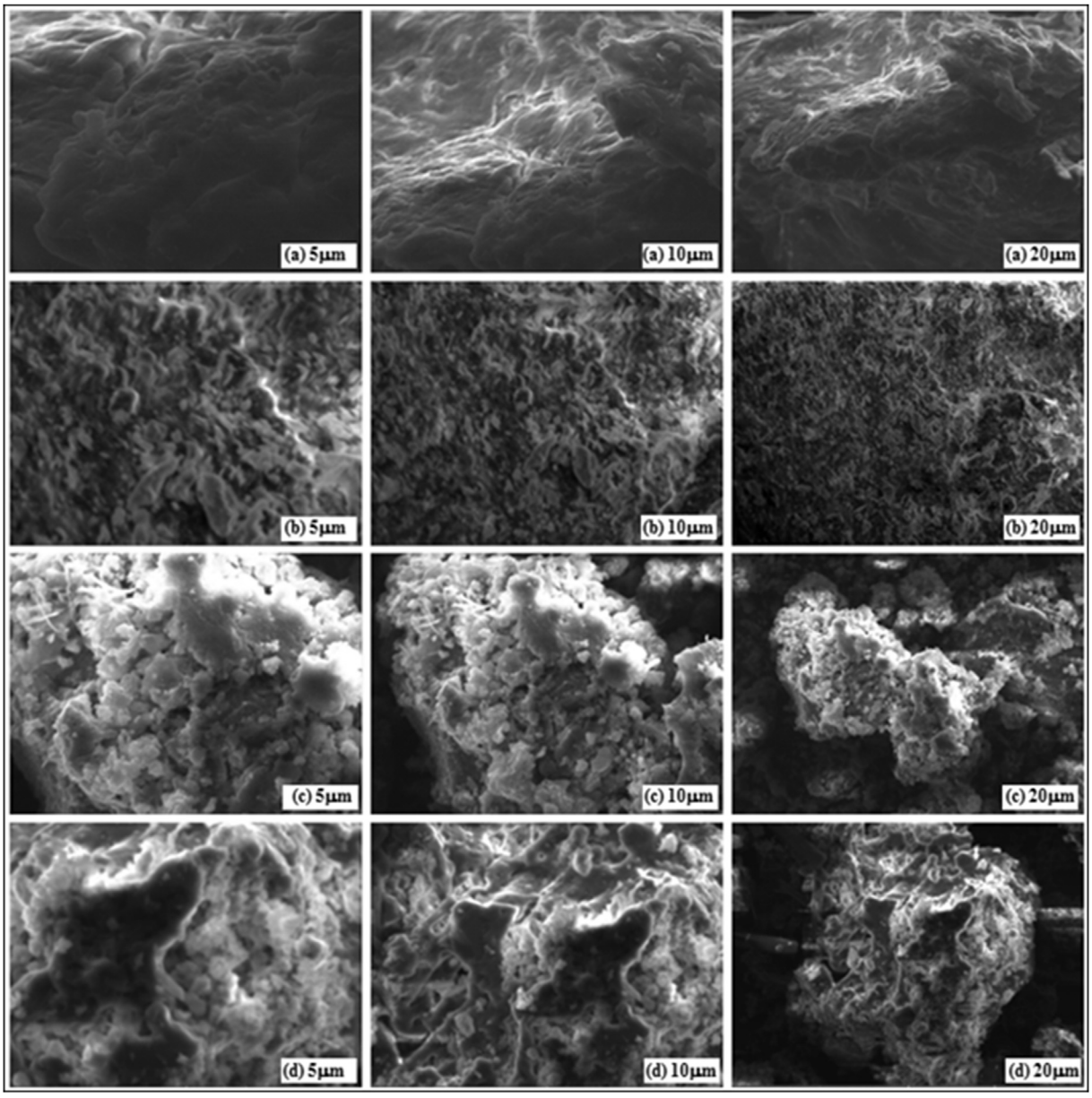

Figure 15. Scanning Electron Microscope (SEM) analysis with magnification 5µm, 10µm and 20µm for (a): Chitosan FC, (b): Chitosan DCA, (c): Chitosan CA and (d): Chitosan NA.

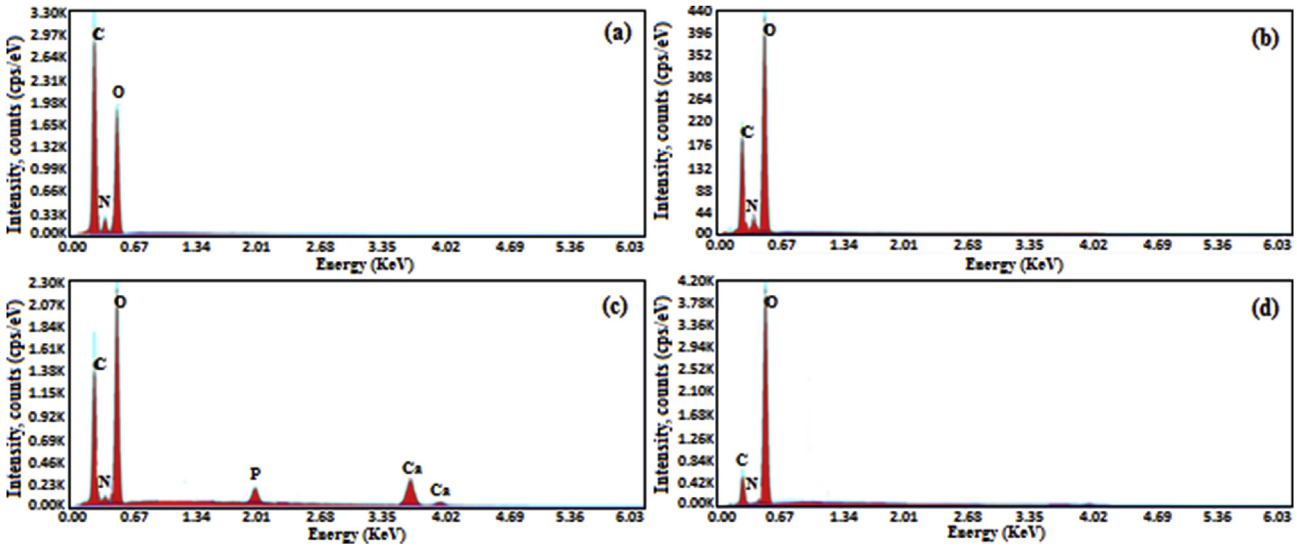

Figure 16. EDX spectrum analysis for (a): Chitosan FC, (b): Chitosan CA, (c): Chitosan DCA and (d): Chitosan NA.

destruction. Finally, the mass is lost by 2.65% in range of temperature 840 and 1030 °C with DTG maximum peak at 1000 °C, after mineral part recrystallization due to rest of calcium and phosphorus and liberation of any last organic substances. Those all analysis shows that a method of chitosan extraction has an effect on their thermal stability. The Chitosan CA is more thermally stable than Chitosan DCA and Chitosan FC, because he loses his mass slowly, after five degradations showing more thermal inertia. All thermal events remarked in TG and DTG analysis are reported in Table 8. All our TG/DTG curves of chitosan are on concordance with those studies of following authors PEREIRA et al [45], ZHENG et al [46] and SAFDAR et al [47].

3.7. Scanning Electron Microscopy

Scanning Electron Microscope SEM is one of most analysis to observe the surface morphology, particles sizes and microstructure of the materials crystals or amorphous polymers. This microscope produce images after scanning the surface of the sample by intense and focused beam of electrons that interact with atoms of materials, producing various signals containing several information concerning the surface topography.

In our case, Scanning electron microscopy (VEGA3 TESCAN, Cadi Ayyad University, Marrakech, Morocco) was used to observe the morphological changes and differences in structure between Chitosan FC, Chitosan DCA, Chitosan CA and Chitosan NA. The surface morphology was taken at an acceleration voltage of 10 kV, by almost working distance (WD) for our samples such as 9.73mm for Chitosan FC, 9.98mm for Chitosan DCA, 10.02mm for Chitosan CA, and 10.05mm for Chitosan NA, with same magnifications: 5 μm, 10 μm and 20 μm respectively for each chitosan samples. All SEM images are regrouped in Figure 15.

The SEM analysis results show an irregularity in Chitosan FC microstructure and its surface morphology: Smooth surface with some rough, irregular membrane fissures, irregular pattern, no pores and no existence of chitosan nanoparticles. The image of the Chitosan DCA reveals that the surface is rough, disordered, disorganized with distorted microstructure with some cracks and very small pores. We notice the appearance also of some smooth and homogenous isolated surface in few areas indicating formation of unacetylated chitosan. The absence of homogeneity in Chitosan DCA surface with smooth part and rough part both is the signs of phase separation indicate the incomplete extraction of the chitosan from shrimp shells. For Chitosan CA and Chitosan NA, We noticed almost similar morphology: Rough surface, irregular block, crystalline cluster with some porosity due to use of ammonium like results of TOLESAet al [48], and an appearance of chitosan nanoparticles. However, we observed some differences between them such as: Appearance of few nanometric threads in Chitosan CA structures, some small smooth and flat zone in Chitosan NA (The same for Chitosan CA but not a lot). We still notice that Chitosan CA nanoparticles sizes are smaller than those of Chitosan NA. Similar results were obtained by S.Salamat et al using sulfuric acid, acetic acid [49].

Generally, we notice that the extraction method of chitosan exhibit changes in the shape and morphology. The chitosan samples which were prepared by concentration acids have a higher specific surface area compared to chitosan prepared by diluted acid or Chitosan FC. Reason that the concentrated acids remove all minerals and impurities from the shrimp shells and forces it for total dissolution in order to generate a lot of chitosan nanoparticles.

3.8. Energy Dispersive X-Ray spectroscopy

Energy Dispersive X-Ray spectroscopy EDX, also noted EDS or EDAX, is an X-Ray non destructive analysis used to identify the elemental composition of materials. Its principle based to convey an external X-ray

Table 9. Elementary EDX analysis for Chitosan DCA, Chitosan FC, Chitosan CA, Chitosan NA.

Sample	Chitosan DCA		Chitosan FC		Chitosan CA		Chitosan NA	
Element	Weight %	Atomic %	Weight %	Atomic %	Weight %	Atomic %	Weight %	Atomic %
C	26,26	35,9	45.55	51.92	29,01	35,55	15,02	18,99
N	4,17	4,89	12.28	12.01	5,22	3,91	3,72	3,89
O	49,1	50,41	42.16	36.08	65,76	60,53	81,25	77,11
P	3,4	1,8	0.00	0.00	0.00	0.00	0.00	0.00
Ca	17,06	6,99	0.00	0.00	0.00	0.00	0.00	0.00

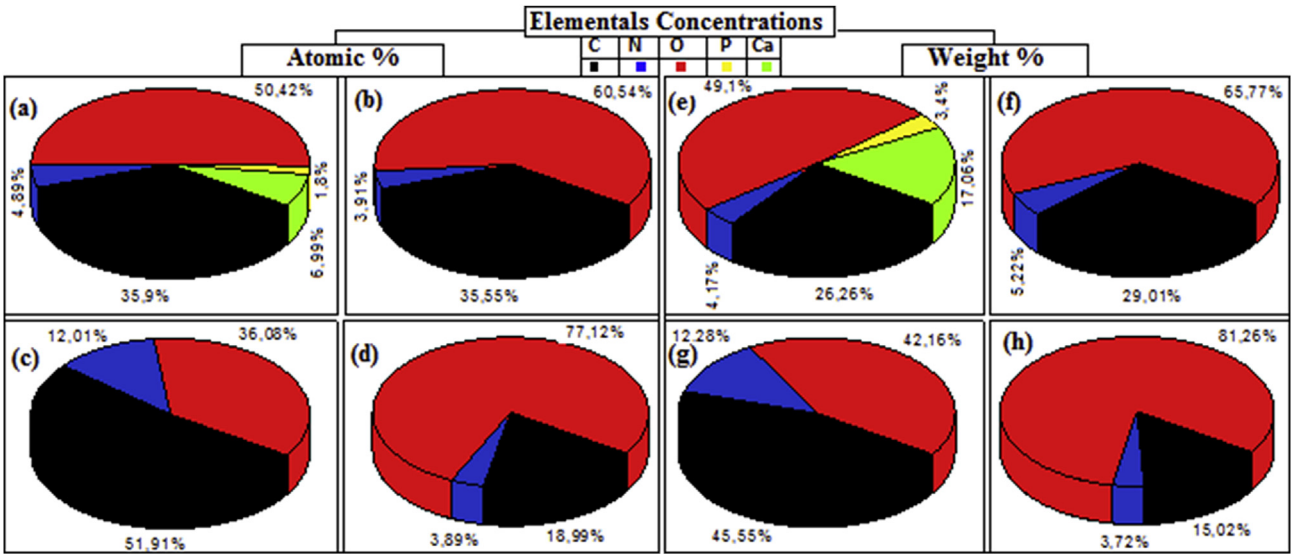

Figure 17. Representation of elemental atomic concentrations for (a): Chitosan DCA, (b): Chitosan CA, (c): Chitosan FC, (d): Chitosan NA. And elementals weight concentrations for (e): Chitosan DCA, (f): Chitosan CA, (g): Chitosan FC, (h): Chitosan NA.

stimulation on electrons of K bands within atoms, in order to one or more this electron leaves its orbit and will be replaced by an electron from L band, with emission of radiation energy kα, this last electron will be also replaced by an electron from M band with emission of Lα radiation energy. Furthermore, the electron of K band can be replaced directly by electron from M band with emission of Kβ radiation energy. All of these energies radiation will be captured by the device's collector and processed in order to displays a spectrum with different peaks. Each peak corresponds to a unique chemical element with its atomic and weight concentration [50]. All EDX spectrum analysis for Chitosan FC, Chitosan DCA, Chitosan CA and Chitosan NA are shown in Figure 16, and the results of each sample elemental composition are summarized in Table 9, and plotted in Figure 17 in order to compare easily the elemental weight and atomic concentration percentages in each chitosan samples. From the results, we notice the presence of the peaks for following element: the carbon C, the nitrogen N and the oxygen O with a different intensities related to their concentration in each chitosan samples. However, the characteristic peaks of the phosphorus P, and the calcium Ca appeared only in Chitosan DCA. This result proves the incapacity of diluted acid to remove all minerals from the shrimp shells, contrary to concentrated acids can maybe leave just a few minerals traces.

4. Conclusion

We can conclude that our chitosans gained by concentrated acids and base, are pure and ultrafine in nanometer scale 8–30 nm with a very good degree of deacetylation (DD) 80%, splendid for water treatment. Also good on opto-electronic performance with small gap valence as semiconductor, give them a possibility to be used for production of intelligent biodegradable fibers. As well, they provide a different degree of crystallinity towards biodegradable sutures. They offer more heat resistance until 367 °C for starting thermal degradation, in comparison to commercial chitosan (from Fluka Chemica Company) which starts degradation at 297 °C.

Our method gives a possibility to produce a big quantity of chitosan in short time duration. It can be also used for treatment of very dirty shrimp shells waste, because the concentrated acids remove all impurity. We recommend to use it only in Laboratories and Factories, and forbidden at home.

Our chitosan samples present are suitable for pharmaceutical applications, due to their purity and high degree of deacetylation.

The grains size obtained of chitosan in our work, is offering good perspective which can be used easily on coating based on carbon nanotude and graphene.

Moreover, these materials can be used as a wound-healing material for the prevention of opportunistic infection and for enabling wound healing, as antibacterial agents, gene delivery vectors and carriers for protein release and drugs.

Declarations

Author contribution statement

Mohammed Eddya: Conceived and designed the experiments; Performed the experiments; Analyzed and interpreted the data; Contributed reagents, materials, analysis tools or data; Wrote the paper.

Bouazza Tbib: Conceived and designed the experiments; Performed the experiments.

Khalil El-Hami: Conceived and designed the experiments; Analyzed and interpreted the data; Contributed reagents, materials, analysis tools or data.

Funding statement

This research did not receive any specific grant from funding agencies in the public, commercial, or not-for-profit sectors.

Competing interest statement

The authors declare no conflict of interest.

Additional information

No additional information is available for this paper.

Acknowledgements

Special thanks to Prof. Dr. Abdelkader Outzourhit and Rachid El-Moutamanni from Cadi Ayyad University, Marrakech Morocco for SEM-EDX tools analysis, without forgetting Prof. Patricia Moita from University of Evora, Portugal for TG-DTG apparatus. Special thanks to dear Abderahim HASRI from Hassan I University of Settat, Morocco for XRD and XRF apparatus.

References

[1] Xiaoyun Li, Meihu Ma, Dong Ahn, et al., Preparation and characterization of novel eggshell membrane-chitosan blend films for potential wound-care dressing: from waste to medicinal products, Int. J. Biol. Macromol. 123 (2019) 477–484.

[2] P.V. Nageswararao, D.E. Babu, Assessment of Anti-microbial Activity of Chitin, Chitosan and Shrimp Shell of Litopenaeus Vannamei from Bhimavaram Farms, West Godavari District, Andhra Pradesh, 2019.

[3] Shahia Khattak, Fazli Wahid, Ling-Pu Liu, et al., Applications of cellulose and chitin/chitosan derivatives and composites as antibacterial materials: current state and perspectives, Appl. Microbiol. Biotechnol. 103 (5) (2019) 1989–2006.

[4] R. Salah, P. Michaud, F. Mati, et al., Anticancer activity of chemically prepared shrimp low molecular weight chitin evaluation with the human monocyte leukaemia cell line, THP-1, Int. J. Biol. Macromol. 52 (2013) 333–339.

[5] M. Bouhenna, R. Salah, R. Bakour, et al., Effects of chitin and its derivatives on human cancer cells lines, Environ. Sci. Pollut. Control Ser. 22 (20) (2015) 15579–15586.

[6] M.S. Benhabiles, N. Abdi, N. Drouiche, et al., Protein recovery by ultrafiltration during isolation of chitin from shrimp shells Parapenaeus longirostris, Food Hydrocolloids 32 (1) (2013) 28–34.

[7] S.E. Darmon, K.M. Rudall, Infra-red and X-ray studies of chitin, Discuss. Faraday Soc. 9 (1950) 251–260.

[8] Jack G. Winterowd, Paul A. Sandford, Chitin and Chitosan, Food Science and Technology-New York-Marcel Dekker, 1995, p. 441.

[9] F. Hoppe-seyler, Ueber chitin und cellulose, Ber. Dtsch. Chem. Ges. 27 (3) (1894) 3329–3331.

[10] Nitar Nwe, Tetsuya Furuike, Hiroshi Tamura, Chitosan from aquatic and terrestrial organisms and microorganisms: production, properties and applications. Biodegradable Materials: Production, Properties and Applications, Nova Science, Hauppauge, NY, 2011, pp. 29–50.

[11] Vijay S. Yeul, Sadhana S. Rayalu, Unprecedented chitin and chitosan: a chemical overview, J. Polym. Environ. 21 (2) (2013) 606–614.

[12] J.L. Lassaigne, Mémoire sur un Procède Simple pour Constater la Présence de lAzote dans des Quantités Minimes de Matière Organique, Compt Rendus 16 (1843) 387–391.

[13] R. Rajasree, K.P. Rahate, An overview on various modifications of chitosan and it's applications, Int. J. Pharma Sci. Res. 4 (11) (2013) 4175.

[14] Riccardo AA. Muzzarelli, Joseph Boudrant, Diederick Meyer, et al., Current views on fungal chitin/chitosan, human chitinases, food preservation, glucans, pectins and inulin: a tribute to Henri Braconnot, precursor of the carbohydrate polymers science, on the chitin bicentennial, Carbohydr. Polym. 87 (2) (2012) 995–1012.

[15] Kishore D. Rane, Dallas G. Hoover, An evaluation of alkali and acid treatments for chitosan extraction from fungi, Process Biochem. 28 (2) (1993) 115–118.

[16] Aline Percot, Christophe Viton, Alain Domard, Optimization of chitin extraction from shrimp shells, Biomacromolecules 4 (1) (2003) 12–18.

[17] Felicity Burrows, Clifford Louime, Michael Abazinge, et al., Extraction and evaluation of chitosan from crab exoskeleton as a seed fungicide and plant growth enhancer, Am.-Eurasian J. Agric. Environ. Sci. 2 (2) (2007) 103–111.

[18] Ahmed A. Tayel, Shaaban H. Moussa, F. Wael, et al., Antimicrobial textile treated with chitosan from Aspergillus Niger mycelial waste, Int. J. Biol. Macromol. 49 (2) (2011) 241–245.

[19] V. Ghormade, E.K. Pathan, M.V. Deshpande, Can fungi compete with marine sources for chitosan production? Int. J. Biol. Macromol. 104 (2017) 1415–1421.

[20] Osama M. Darwesh, Yousef Y. Sultan, Mohamed M. Seif, et al., Bio-evaluation of crustacean and fungal nano-chitosan for applying as food ingredient, Toxicology Reports 5 (2018) 348–356.

[21] Surinder Kaur, Gurpreet Singh Dhillon, The versatile biopolymer chitosan: potential sources, evaluation of extraction methods and applications, Crit. Rev. Microbiol. 40 (2) (2014) 155–175.

[22] Hassiba Laribi-Habchi, Amel Bouanane-Darenfed, Nadjib Drouiche, et al., Purification, characterization, and molecular cloning of an extracellular chitinase from Bacillus licheniformis stain LHH100 isolated from wastewater samples in Algeria, Int. J. Biol. Macromol. 72 (2015) 1117–1128.

[23] Burkhard Beckhoff, Birgit Kanngießer, Norbert Langhoff, et al. (Eds.), Handbook of Practical X-ray Fluorescence Analysis, Springer Science & Business Media, 2007.

[24] Meredith Eggers Ostrom, Separation of clay minerals from carbonate rocks by using acid, J. Sediment. Res. 31 (1) (1961) 123–129.

[25] Mohammad R. Kasaai, A review of several reported procedures to determine the degree of N-acetylation for chitin and chitosan using infrared spectroscopy, Carbohydr. Polym. 71 (4) (2008) 497–508.

[26] J. Brugnerotto, J. Lizardi, F.M. Goycoolea, et al., An infrared investigation in relation with chitin and chitosan characterization, Polymer 42 (8) (2001) 3569–3580.

[27] Z. Abdeen, Somaia G. Mohammad, Study of the adsorption efficiency of an eco-friendly carbohydrate polymer for contaminated aqueous solution by organophosphorus pesticide, Open J. Org. Polym. Mater. 2014 (2013).

[28] N.G. Das, P.A. Khan, Z. Hossain, Chitin from the shell of two coastal portunid crabs of Bangladesh, Indian J. Fish. 43 (4) (1996) 413–415.

[29] S. Qazi, S. Junaid, Adrian R. Rennie, Jeremy K. Cockcroft, et al., Use of wide-angle X-ray diffraction to measure shape and size of dispersed colloidal particles, J. Colloid Interface Sci. 338 (1) (2009) 105–110.

[30] N. Thirunavukkarasu, Biology, Nutritional Evaluation and Utilization of Mud Crab Scylla Tranquebarica (Fabricius, 1798), Thèse de doctorat. Ph. D. Thesis, Annamalai University, India, 2005.

[31] Nils Almqvist, Fractal analysis of scanning probe microscopy images, Surf. Sci. 355 (1-3) (1996) 221–228.

[32] N.R. Taskar, V. Natarajan, I.V. Bhat, S.K. Gandhi, J. Cryst. Growth 86 (1980) 288.

[33] Nevill Francis Mott, Edward A. Davis, Electronic Processes in Non-crystalline Materials, Oxford university press, 2012.

[34] Silvia Bautista-Baños, Ana Niurka Hernandez-Lauzardo, Miguel Gerardo Velazquez-del Valle, et al., Chitosan as a potential natural compound to control pre and postharvest diseases of horticultural commodities, Crop Protect. 25 (2) (2006) 108–118.

[35] Dilyana Zvezdova, Synthesis and characterization of chitosan from marine sources in Black Sea, in: Annual Proceedings," Angel Kanchev" University of Ruse 49, 2010, pp. 65–69, no 9.1.

[36] P. Sugumaran, V. Priya Susan, P. Ravichandran, et al., Production and characterization of activated carbon from banana empty fruit bunch and Delonix regia fruit pod, J. Sustain. Energy Environ. 3 (3) (2012) 125–132.

[37] M. Soundarrajan, T. Gomathi, P.N. Sudha, Understanding the adsorption efficiency of chitosan coated carbon on heavy metal removal, Int. J. Sci. Res. Publ 3 (1) (2013) 1–10.

[38] Ana I. Carrapiso, Carmen García, Development in lipid analysis: some new extraction techniques and in situ transesterification, Lipids 35 (11) (2000) 1167–1177.

[39] ABDOU, S. Entsar, Khaled SA. Nagy, Maher Z. Elsabee, Extraction and characterization of chitin and chitosan from local sources, Bioresour. Technol. 99 (5) (2008) 1359–1367.

[40] L.F.C. Oliveira, P.S. Santos, Chromophore-selective resonance Raman spectra of copper (II) croconate and rhodizonate complexes with nitrogenous counterligands, J. Mol. Struct. 263 (1991) 59–67.

[41] Georgia MA. Junqueira, Willian R. Rocha, de Almeida, B. Wagner, et al., Theoretical study of oxocarbons: structure and vibrational spectrum of the D6h and C2 forms of the rhodizonate ion, J. Mol. Struct.: THEOCHEM 684 (1-3) (2004) 141–147.

[42] A. Zając, J. Hanuza, M. Wandas, et al., Determination of N-acetylation degree in chitosan using Raman spectroscopy, Spectrochim. Acta Mol. Biomol. Spectrosc. 134 (2015) 114–120.

[43] Tiverios C. Vaimakis, Thermogravimetry (TG) or Thermogravimetric Analysis (TGA), University of Ioannina, 2013.

[44] F. Paulik, Thermal analysis under quasi-isothermal–quasi-isobaric conditions, Thermochim. Acta 340 (1999) 105–116.

[45] Leudimar Aires Pereira, Luizângela Da Silva Reis, Felipe Alves Batista, et al., Biological Properties of Chitosan Derivatives Associated with the Ceftazidime Drug, Carbohydrate Polymers, 2019, p. 115002.

[46] Feng-Yi Zheng, Ruisong Li, Jiadan Hu, et al., Chitin and waste shrimp shells liquefaction and liquefied products/polyvinyl alcohol blend membranes, Carbohydr. Polym. 205 (2019) 550–558.

[47] Rizwan Safdar, Nirmala Gnanasundaram, Regupathi Iyyasami, et al., Preparation, characterization and stability evaluation of ionic liquid blended chitosan tripolyphosphate microparticles, J. Drug Deliv. Sci. Technol. 50 (2019) 217–225.

[48] Leta Deressa Tolesa, Bhupender S. Gupta, Ming-Jer Lee, Chitin and chitosan production from shrimp shells using ammonium-based ionic liquids, Int. J. Biol. Macromol. 130 (2019) 818–826.

[49] Samaneh Salamat, Mojtaba Hadavifar, Hassan Rezaei, Preparation of nanochitosan-STP from shrimp shell and its application in removing of malachite green from aqueous solutions, J. Environ. Chem. Eng. 7 (5) (2019) 103328.

[50] T.C. Lovejoy, Q.M. Ramasse, M. Falke, et al., Single atom identification by energy dispersive X-ray spectroscopy, Appl. Phys. Lett. 100 (15) (2012) 154101.